NOTES AND CORRESPONDENCE

Effects of a Mountain Wave Windstorm at the Surface

CARL F. DIERKING

National Weather Service Forecast Office, Juneau, Alaska

14 March 1997 and 26 January 1998

ABSTRACT

A mountain wave windstorm in 1993 is documented for the Taku River Valley near Juneau, Alaska. The mountain wave produces a mesoscale pressure response that appears to enhance local gap flow and complicates efforts to separate the two forcing mechanisms. In addition, the Nested Grid Model is evaluated in terms of its ability to predict atmospheric structure favorable for the development of a mountain wave, since current model resolutions are not small enough to predict the event itself. In the 1993 case, numerical guidance is shown to have some value in the prediction of an atmospheric state conducive to the development of the windstorm.

1. Introduction

The steep mountainous terrain southeast of Juneau, Alaska, and the adjacent Taku River valley (Figs. 1 and 2) are contributors to the spectacular downslope windstorm known locally as the ''Taku'' (Colman and Dierking 1992). Although the most intense winds are associated with the wave itself, there is a complex interaction between the wave and surface pressure in the Taku valley that appears to enhance gap flow during these events. It is likely that many other downslope windstorms occur with similar complexity. The Cooperative Program for Operational Meteorology, Education and Training (COMET), with investigators from the University of Washington and the National Weather Service, Juneau, Alaska, examined in detail several windstorm events during the 1992/93 winter. In particular, the study focused on mountain-wave-induced flow and surface pressure effects, in search of a better description of the mesoscale process. Also examined is the ability of the Nested Grid Model (NGM), a synoptic-scale model, to predict atmospheric conditions favorable for mountain wave development.

2. Methodology

a. Wave theory and Taku winds

The Taku wind was most recently examined by Colman and Dierking (1992), who concluded that it is the product of an amplified mountain wave, which is well documented as the source of many mountain windstorms.

Linear theory was used by Klemp and Lilly (1975) to suggest that vertically propagating waves were reflected by variations in atmospheric stability and amplified through constructive reinforcement (superposition). Later Klemp and Lilly (1978) used a nonlinear model to show that wave reflection and amplification can occur when a level of zero cross-barrier wind flow or flow reversal is present. This is called the ''critical level.'' Peltier and Clark (1979) showed that even when a critical level is not present in the mean atmospheric state, the possibility exists for a growing wave to overturn and generate its own ''self-induced'' critical level resulting in stronger wave amplification.

Other work by Durran (1986, 1990), Smith (1985), Smith and Sun (1987) used hydraulic theory as an analog for downslope winds to demonstrate that wave development was sensitive to the presence of an inversion or strong gradients in static stability. In the hydraulic analog, dense cold air below an inversion develops strong downstream flow as it traverses a mountain when there is a transition from subcritical to supercritical flow.

For Taku winds, the wave develops when northeasterly offshore flow is funneled through a gap in the Coast Mountain Range created by the Taku River valley and forced over Salisbury Ridge (Figs. 2 and 3). Colman and Dierking (1992) concluded that in addition to the cross-barrier flow, a mean-state critical level and strong static stability were necessary conditions to promote development of a mountain wave and produce Taku winds at the surface. Initially pressures fall and winds increase near the ridge top. As the wave intensifies, pressure falls extend down the lee side of the mountain and winds at the surface become increasingly severe.

Corresponding author address: Dr. Carl F. Dierking, National Weather Service, P.O. Box 32179, Juneau, AK 99801-0618.
E-mail: carl.dierking@noaa.gov

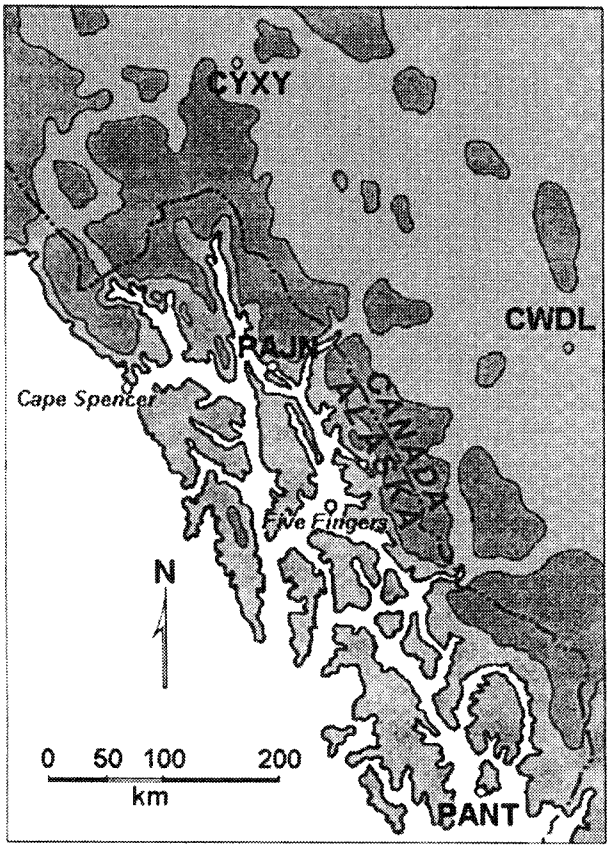

FIG. 1. Topography and station locations for southeast Alaska and parts of northwest Canada. Darker shading identifies terrain elevations above 1500 m.

These general conditions were narrowed somewhat to be more specific for the Taku; however, due to the lack of observed data in the affected area, the degree to which this could be done was limited. Typically the inversion occurs between 1500 and 2000 m above mean sea level (MSL), cross-barrier flow is at least 15–20 m s^{-1} from the northeast, and a mean-state critical level is found between 3000 and 5500 m MSL. A comparison of the observed mesoscale changes at the surface during Taku events with model initializations and forecasts may help to refine these criteria.

There is more than one synoptic pattern that can lead to an atmospheric state conducive to Taku development. Colman and Dierking (1992) described two synoptic variations (cyclonic and anticyclonic) that satisfied the three conditions for Taku winds. An Arctic air mass from northwest Canada invading the lower levels or warm maritime air just above the surface from an approaching warm front can both produce strong low-level stability. There are also several favored locations for fronts or pressure centers, which increase northeasterly wind components for cross-barrier flow.

Although the critical level requires a more restrictive synoptic condition to produce the necessary vertical wind profile, this too can be accomplished in different ways. For Salisbury Ridge, which runs from northwest to southeast, a strong northeast cross-barrier component at lower levels can decrease to zero at the height of the upper trough or in northwest flow from an upper ridge. An east wind component from an approaching front will decrease to zero as winds veer with height due to the trough aloft.

In general, a change in atmospheric conditions away from the established criteria would reduce support for maintaining the mountain wave and lead to a cessation of downslope winds at the surface. However, it is possible that there are occasions when wave overturning prolongs the critical-level condition past the time that it would exist as a mean atmospheric state.

b. Wave-induced flow versus gap flow

Downslope windstorms like the Taku require a more specialized atmospheric state than the more common ''gap wind,'' which is a flow of air accelerated under the influence of a pressure gradient in the along-gap direction. Gap winds are prevented from attaining geostrophic balance by the higher terrain on either side of the gap. Overland and Walter (1981) showed that these winds reach an approximate ageostrophic balance between inertial forces and the gap-parallel pressure gradient when the length of the gap is much greater than the width. Also, the width of the gap must be less than one Rossby radius.

In southeast Alaska, it is well known that most local boundary layer winds flow parallel to the channels and are related to the along-channel pressure gradient. Empirical rules relating the gap-parallel pressure gradient to surface winds are generally successful. However, they are not helpful in the case of the Taku, where the wind flow is not in the along-gap direction, but across the channel and perpendicular to Salisbury Ridge (Fig. 2).

In the vicinity of Juneau, strong offshore pressure gradients and gap flow are quite common, and they usually accompany Taku winds. Typically the downslope winds are in a cross-channel direction opposite the steeper terrain of Salisbury Ridge, while the gap flow is parallel to local channels and mountain passes. At times during Taku events, minor gaps through Salisbury Ridge may also experience an increase in wind, making the mountain-wave-induced flow difficult to isolate from nearby gap flow. The downslope winds, however, are generally stronger and opposite the steeper terrain.

c. Field measurements

In the late summer of 1992, supplemental instruments were placed at locations considered crucial for a better surface description of the Taku. Figure 2 shows the location of existing National Weather Service (NWS) observations along with the new sites. The NWS observations included sea level pressure and wind, except for

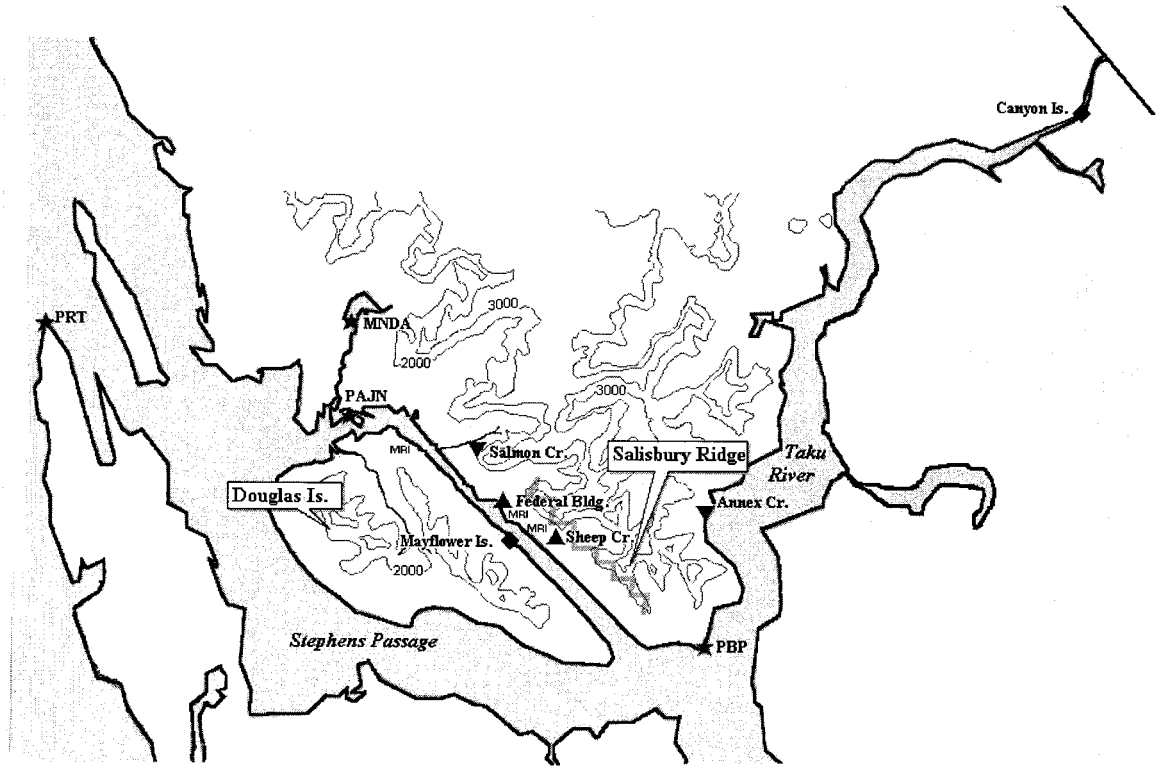

FIG. 2. Topography of the area surrounding Juneau with elevation contours at 2000 ft (600 m) and 3000 ft (900 m). Observation sites are shown with stars designating operational NWS points. Supplemental observations are depicted with triangles for sites with anemometers, inverted triangles for sites with microbarographs, and squares for sites with both.

Point Bishop (PBP), which was an automated instrument that was not equipped with a pressure sensor. Recording barographs were placed at Mayflower Island, Salmon Creek Dam, Annex Creek, and Canyon Island. Anemometers were made available at Sheep Creek and Canyon Island. The Meteorology Research, Inc. portable instrument platforms were located at three additional sites for recording wind run and temperature.

d. Synoptic and mesoscale analyses

When Taku winds were observed, synoptic analyses of surface pressure from the National Centers for Environmental Prediction were compared with locally analyzed mesoscale analyses. The mesoscale analyses utilized the microbarograph pressures to supplement existing NWS observations. Since the barographs were in remote sites and could not be calibrated routinely, two types of pressure corrections had to be applied, one for pressure values at sea level and the other for time. Both corrections were derived from comparisons with surrounding calibrated instruments. Sea level corrections were determined during periods when the pressure distribution was relatively weak and time corrections were estimated by coordinating the occurrence of high and low peaks in the pressure trend. Since Mayflower Island, Annex Creek, and Canyon Island are close to sea level, most corrections at these sites were relatively small. All

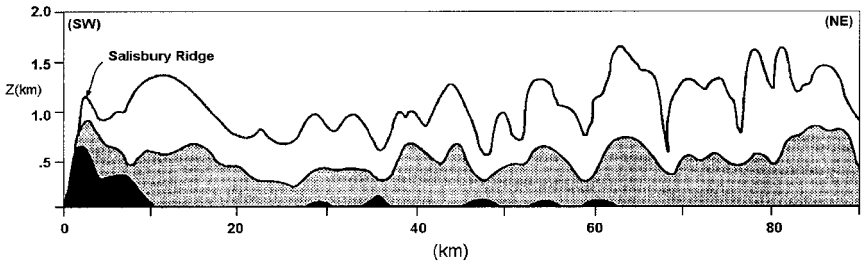

FIG. 3. Elevation cross sections extending northeast from Salisbury Ridge. Shown are the maximum (silhouette), the average (light shading), and the lowest (dark shading) elevations from four equally spaced sections along the ridge.

corrections were applied uniformly throughout the period of focus. These corrected pressures were considered sufficiently accurate for the mesoscale analysis since local pressure trends were more important than individual pressure values.

Unfortunately, the number of Taku events during the winter of 1992/93 was fairly low. Two windstorms did occur but they were weak by historical standards. The strongest occurred on 8 February, when wind gusts at Mayflower Island (on the lee side of Salisbury Ridge) reached 29 m s^{-1} (57 kt) and an anemometer nearly halfway up Salisbury Ridge on Sheep Creek reached 45 m s^{-1} (88 kt). A weak frontal trough preceded the event, which was ideal for determining both types of corrections to the supplemental microbarographs. It is this event that will be the focus of the following case study.

3. Case study: 8 February 1993

At 0000 UTC on 7 February 1993, a weak occluded front, approaching from the southwest, reached Juneau concurrently as high pressure began building northward over the Copper River Basin in interior Alaska. By 0000 UTC 8 February (Fig. 4a), most of the Alaska panhandle was under the influence of high pressure. The center of the high moved eastward and by 0600 UTC was centered over the southern Yukon Territory (Fig. 4b) where it persisted for another 12 h. After 1800 UTC 8 February, high pressure intensified farther east along the Canadian Arctic coast and weakened in the southern Yukon Territory. This resulted in a gradual relaxation of the offshore pressure gradient across southeast Alaska (Figs. 4e,f).

A comparison is made between the series of synoptic-scale charts (Figs. 4a–f) and mesoscale analyses (Figs. 5a–f) for corresponding dates and times spanning the time period of 8 and 9 February 1993. Between 0000 and 1800 UTC on 8 February the mesoscale surface pressure field increasingly deviates from the synoptic-scale analyses. Pressures are substantially lower over Douglas Island causing extreme tightening of the pressure field across Salisbury Ridge and into the Taku River valley. Of particular importance is the intensification of the pressure gradient in the lower end of the Taku River by 1800 UTC on 8 February.

An examination of 3-h pressure changes (Fig. 6) illustrates the above-described pressure gradient increase at the surface. After 1000 UTC, pressures were falling at the Juneau airport and Mayflower Island (on the lee side of Salisbury Ridge) more than twice as fast as at the Annex Creek site on the windward side. Between 1800 and 2000 UTC, the pressure falls at Mayflower Island doubled that of the airport. A comparison of the pressure traces from Annex Creek and Mayflower Island (Fig. 7) reveals significant differences during individual hours, despite similar trends overall. It is apparent that a mesoscale process is lowering pressures with extreme variability on the lee side of the mountain and not the windward side.

Figure 8 dramatically illustrates the scale of change that took place in the surface pressure field. Salisbury Ridge is located between both sets of end points used for gradient calculations. Dease Lake and Juneau are 265 km apart, while Annex Creek and Mayflower Island are separated by only 18 km. The dashed high–low curves between 1700 and 2200 UTC highlight the variability of the pressure gradient across Salisbury Ridge during the time of the strongest winds. This was almost entirely due to the variability of the pressure at Mayflower Island (Fig. 7).

Although winds were extremely gusty on the lee side of Salisbury Ridge, the graph of maximum hourly wind speeds from nearby anemometers (Fig. 9) shows trends that are similar to that of the mesoscale pressure gradient. This is especially true at Mayflower Island and Sheep Creek where winds peaked near the time of the peak in the pressure gradient. A comparison of the two graphs makes it easy to see how an event of this type could go unnoticed in the synoptic scale, yet produce impressive local wind conditions.

Variations in wind and surface pressure on the lee side of the mountain ridge during this event match the findings of Brinkman (1974) who compared detailed surface wind and pressure observations with cross-sectional analyses from two instrumented aircraft during the 22 January 1971 wind storm in Boulder, Colorado. She concluded that the surface wind and pressure variability was the result of a shifting lee trough. Similarly, the radical fluctuations of pressure and wind at Mayflower Island seem to reflect the dynamic nature of the vertical wave aloft.

Three of the wind plots are from anemometers on the lee side of Salisbury Ridge, but the fourth, Canyon Island, was located upstream of the ridge in the Taku River valley. Although not as strong, the trend of the wind at Canyon Island is similar to that of the other sites, despite its position upstream of the ridge in the Taku River valley. This illustrates the difficulty in isolating downslope and gap winds during a mountain wave event since both can be affected.

4. Evaluation of model guidance

The challenge in forecasting a mountain-wave-induced windstorm is to evaluate synoptic-scale guidance in terms of criteria relevant to the mesoscale. Some variables, such as surface pressure, must be closely resolved to predict the mesoscale event while others, such as static stability and cross-barrier flow, may imply synoptic-scale conditions conducive to the occurrence of the event. Although newer operational models, such as the Eta, have more than twice the grid resolution of the NGM, they are still only capable of providing guidance relating to the broadscale synoptic patterns used to identify potential weather situations that might lead to downslope wind

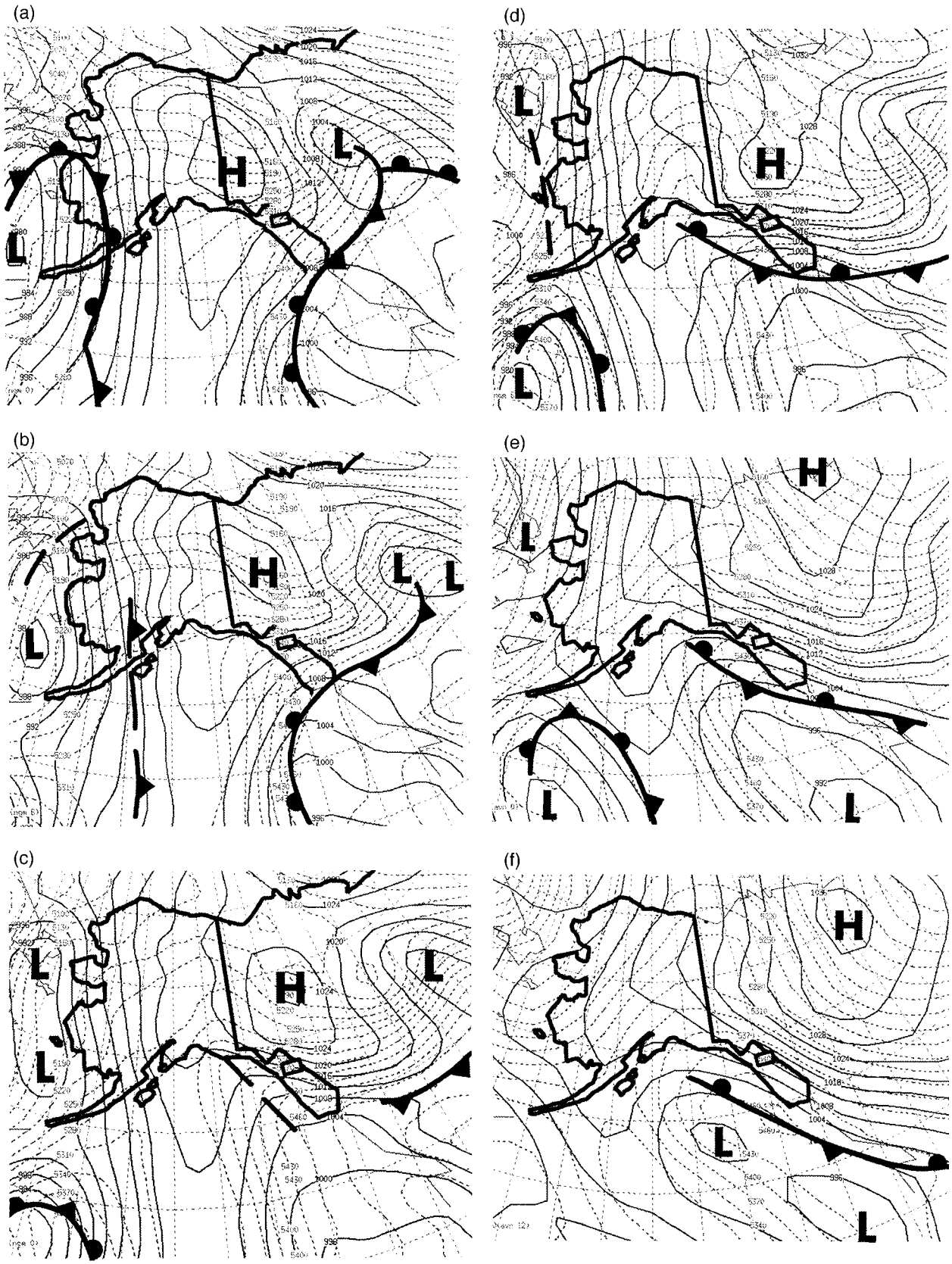

FIG. 4. Sea level pressure (solid), 1000–500-mb thickness (dashed), and frontal analyses for (a) 0000 UTC 8 Feb 1993, (b) 0600 UTC 8 Feb 1993, (c) 1200 UTC 8 Feb 1993, (d) 1800 UTC 8 Feb 1993, (f) 0000 UTC 9 Feb 1993, and (g) 1200 UTC 9 Feb 1993.

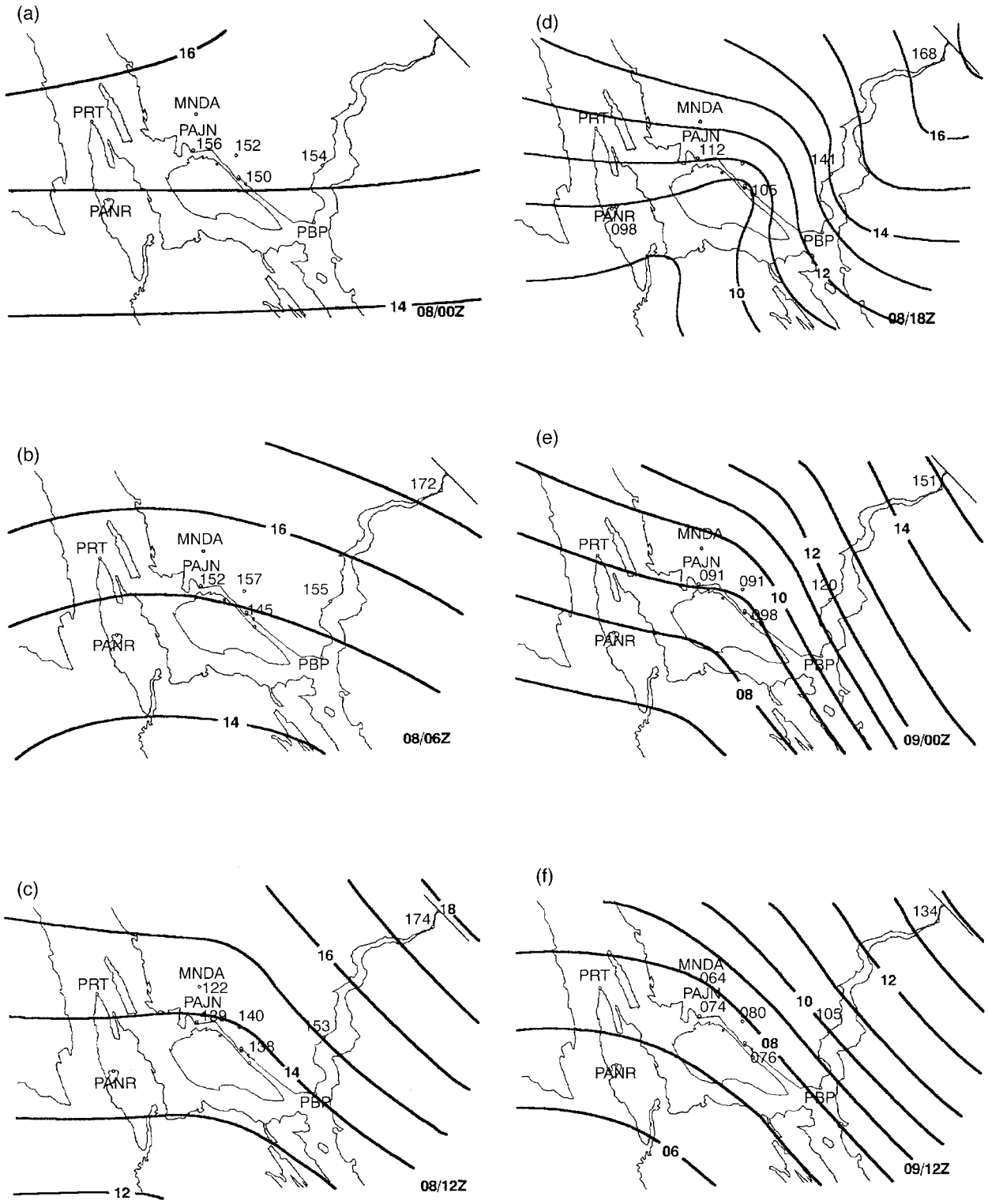

FIG. 5. Mesoscale sea level pressure analyses at (a) 0000 UTC 8 Feb 1993, (b) 0600 UTC 8 Feb 1993, (c) 1200 UTC 8 Feb 1993, (d) 1800 UTC 8 Feb 1993, (f) 0000 UTC 9 Feb 1993, and (g) 1200 UTC 9 Feb 1993.

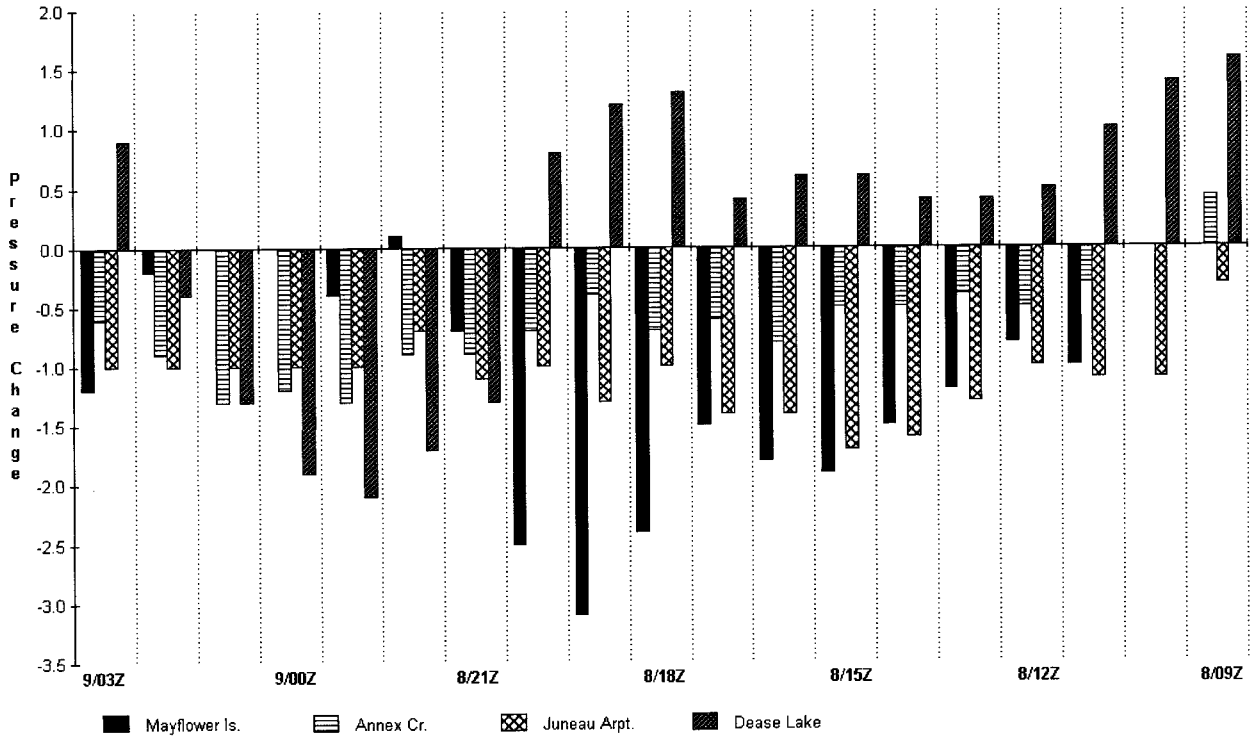

FIG. 6. The 3-h pressure change time series at four locations during the 8 February 1993 Taku wind event. Time increases from right to left.

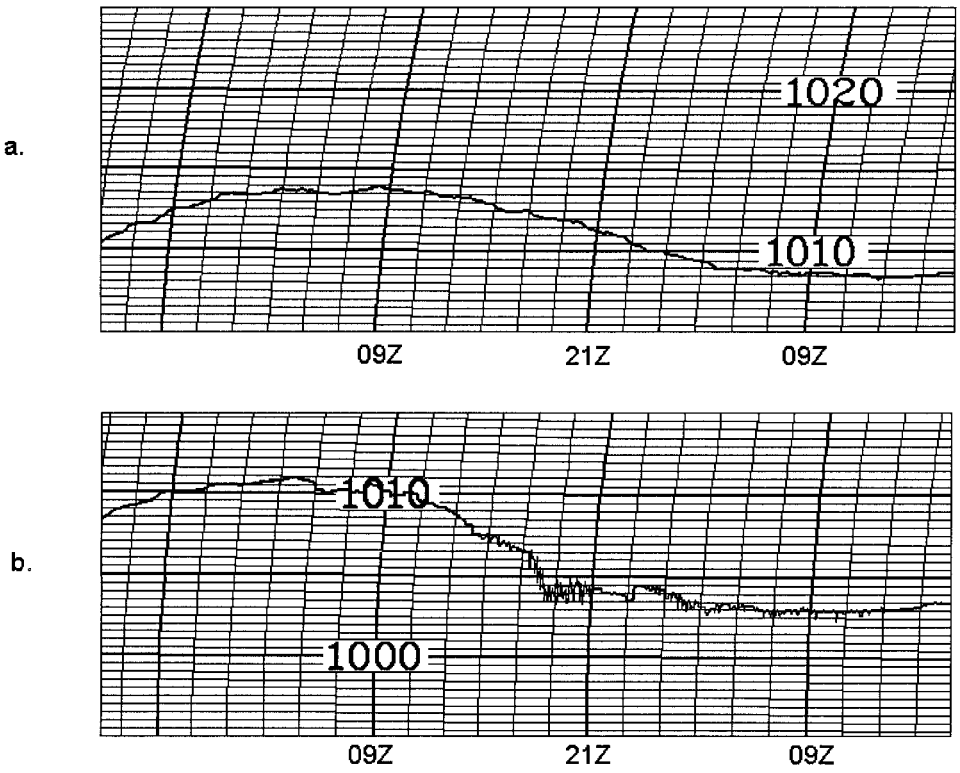

FIG. 7. Microbarograph trace during 8 February 1993 Taku wind for (a) Annex Creek (on windward side of Salisbury Ridge) and (b) Mayflower Island (on lee side of ridge).

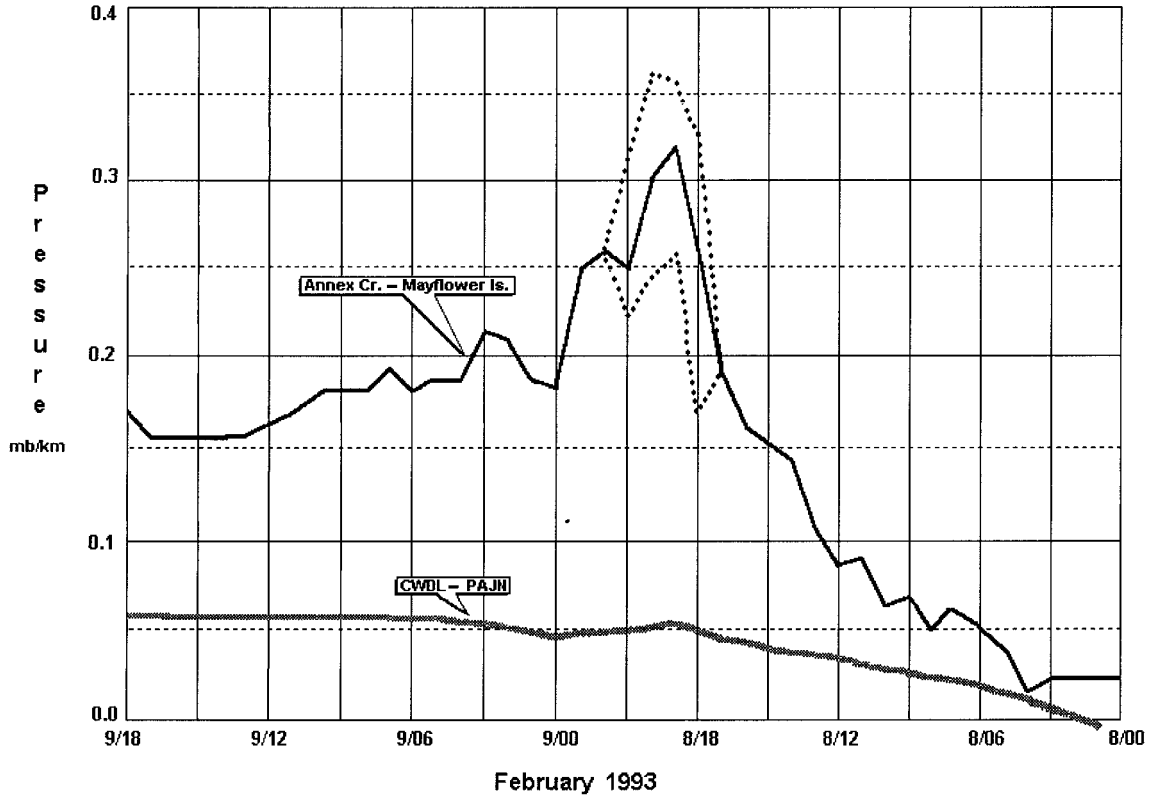

FIG. 8. Pressure gradient (mb km^{-1}) between Mayflower Island and Annex Creek (solid) and between Juneau and Dease Lake (dashed) during 8 February 1993. The split line for Mayflower Island–Annex Creek marks the highest and lowest gradient during that hour.

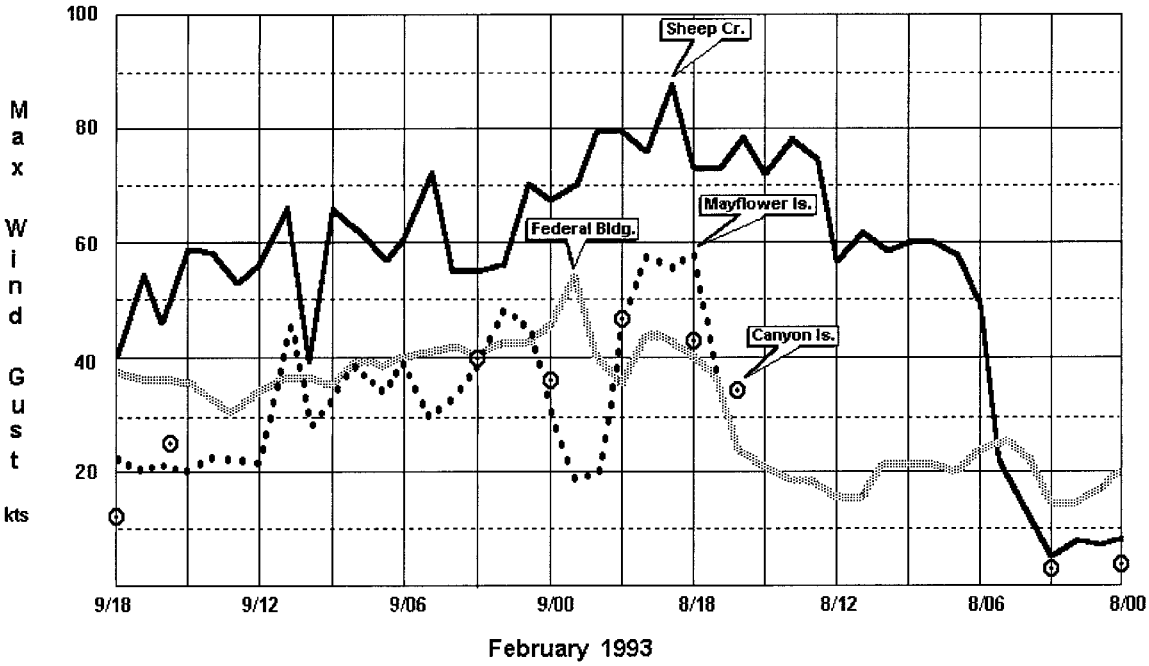

FIG. 9. Maximum wind gusts during 8 February 1993 Taku wind for Sheep Creek (solid), Mayflower Island (dotted), downtown Juneau (gray), and Canyon Island (circled points).

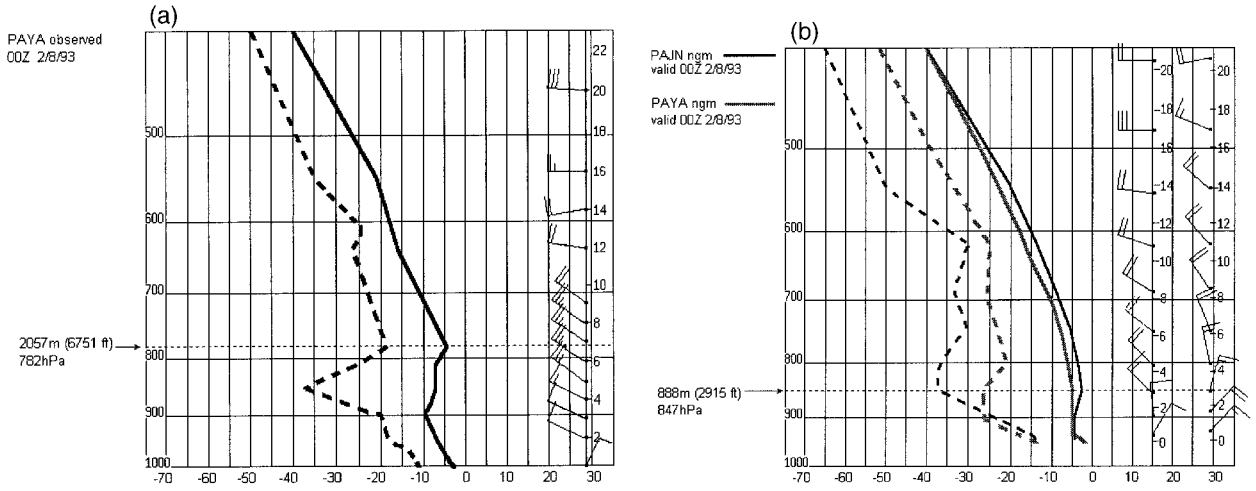

FIG. 10. (a) Yakutat rawinsonde for 0000 UTC 8 February 1993 compared with (b) NGM initialization for Juneau (bold) and Yakutat (normal) both valid at the same time as the sounding.

conditions. Evidence of the 8 February windstorm in the pressure field was much smaller scale than the 80-km grid width of the NGM, and mountains the size of Salisbury Ridge are nonexistent in its topographical grid.

Although it may not be possible to consider all of the details for the local Juneau area, the three mountain wave criteria identified by Colman and Dierking (1992) are often representative of a condition that occurs at a large enough scale to be recognized in a model. Each is listed below along with an evaluation of NGM guidance available at 0000 UTC 8 February.

a. Strong low-level stability extending above the ridge top

Typically in the winter, strong high pressure in northwest Canada is accompanied by very cold Arctic air in the lower atmosphere. On 8–9 February most of southeast Alaska and northwest Canada are under the dominance of high pressure, so it is likely that the lower portion of the atmosphere throughout this region is cold and quite stable. The question is whether strong stability extended above Salisbury Ridge, which is approximately 1200 m.

The observed Yakutat sounding at 0000 UTC on 8 February (Fig. 10a) shows evidence of this Arctic influence in the lower levels with an inversion to 2057 m (6750 ft). The initial NGM soundings at Juneau and Yakutat for the 0000 UTC cycle (Fig. 10b) indicate an inversion to 900 m, with a stable lapse rate to 1900 m at both locations. The error in the NGM initialization, likely due to several factors such as low vertical resolution, higher model elevations at the station locations, and weak surface features, results in weaker low-level stability than is observed at Yakutat. The NGM time series plot of theta (Fig. 11a) for that cycle indicates

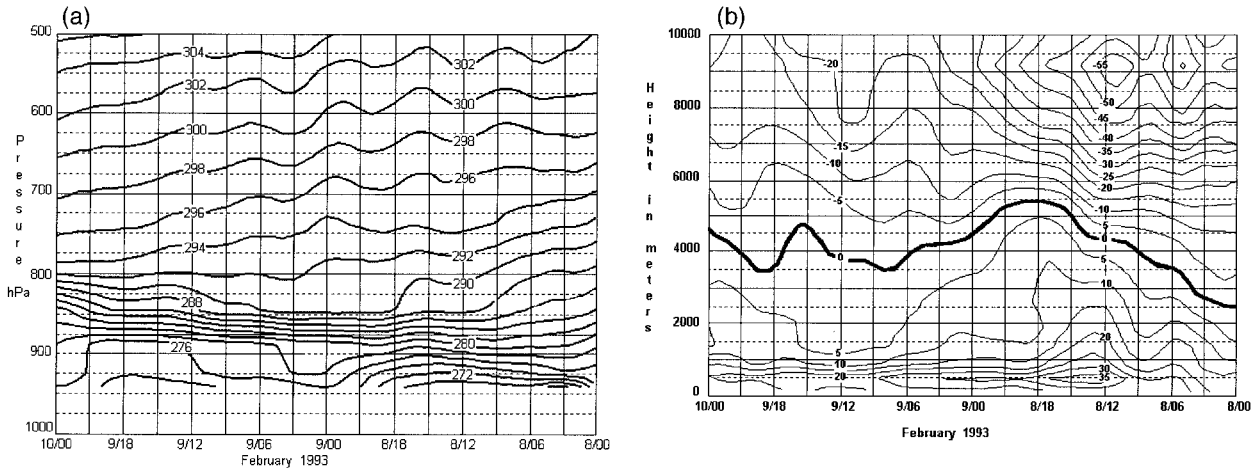

FIG. 11. NGM forecast with respect to mountain wave criteria summarized in two time series displays: (a) theta and (b) magnitude of the wind vector normal to Salisbury ridge (60°) calculated from the 0000 UTC 8 February 1993 run.

that there should be a steady rise in the stable layer through 48 h.

Since the same Arctic air mass was entrenched over much of the region and the initial NGM temperature profiles for Juneau and Yakutat are similar, it would be reasonable to assume the actual height of the stable layer over Juneau is close to that of Yakutat at approximately 2000 m. This suggests that criterion number one was met even before the winds increased significantly. Figures 5–9 show evidence of dramatic changes occurring after 0000 UTC 8 February. Because low-level stability alone is not sufficient for vertical wave development and only gradual change is predicted after 0000 UTC, it is likely there are other changes in the next 24 h that triggered the event.

b. Cross-barrier flow at the top of the mountain ridge

At 1200 m, the top of Salisbury Ridge is near the 850-mb level but not high enough to be completely free of terrain considerations. With high pressure in northwest Canada, air is forced offshore over the Coast Mountains and through gaps such as the Taku River valley. Since Salisbury Ridge lies at right angles to the river, and a portion even projects into the river valley near the mouth, it becomes a barrier to northeast offshore flow. As a result, criterion number two is often met during an Arctic air outbreak. Short-wave features near 850 mb affect wind direction at the ridgetop level resulting in reduction or enhancement of the normal wind component relative to the mountain ridgeline. A weak trough rotating around a low, or a short-wave trough moving through a long-wave anticyclonic flow, are both mechanisms that could increase the offshore component.

In the 8 February event, the synoptic features at 850 mb are similar to those at sea level. As the center of the high moved from the Copper River Basin into Canada, the low-level winds veered from north to northeast and increased in strength through the lower layer. This trend also is predicted by the NGM. The time series plot of the NGM wind component at 60° (Fig. 11b), which is the wind direction perpendicular to the orientation of Salisbury Ridge in the offshore direction, shows an increase through the lower 2000 m between 0000 and 1200 UTC and a gradual decrease after 1800 UTC on 8 February. Although criterion number two occurs as early as 0000 UTC, the time of peak cross-barrier airflow is predicted by the NGM to occur between 1200 and 1800 UTC, which is near the time of occurrence of the windstorm.

c. The cross-barrier (ridge top) wind component decreasing with height to zero (the critical level)

This is the most difficult of the three criteria to evaluate. Numerical mountain wave simulations by Durran and Klemp (1987) show a highly varied wave response to changes in the height of either the critical level or the mountain, and yet precise critical level heights over Salisbury Ridge are unavailable because of the lack of rawinsonde stations upstream from Juneau. Mandatory level analyses from previous Taku wind events consistently have shown the existence of a critical level in the vicinity of 500 mb (Colman and Dierking 1992), but without a complete upstream wind profile, it is impossible to define the limits for ideal critical level heights.

Nonetheless, it is possible to make reasonable predictions of the *change* of critical-level height using model forecasts. The bold line in Fig. 11b marks the level where the NGM wind component at 60° is forecast to be zero. In effect, this is the critical level for Salisbury Ridge. From the plot it is seen that the critical level is predicted to rise from 2400 m at 0000 UTC to above 5000 m at 1800 UTC on 8 February (near 500 mb), followed by lowering heights after that time. In addition, the positive wind speed maximum (offshore flow) below the critical level is accompanied by strong flow reversal with a negative maximum above (onshore flow). Although the accuracy of the critical-level height prediction at any given time is uncertain, in this event the NGM predicted a rise in the critical-level height to an elevation more favorable for mountain wave development at the time of the strongest winds.

Since the NGM indicates critical-level heights should return to a height lower than the historically favored level alter 1800 UTC, the conditions beneficial for continuing downslope winds are expected to be short lived. In fact, by 1800 UTC on 8 February, maximum wind gusts had peaked at all four locations and diminished slowly thereafter.

5. Discussion and conclusions

From available data, it appears that the three criteria considered essential for the amplification of a mountain wave over Salisbury Ridge and the subsequent production of strong surface winds, were met at the time of the Taku wind event on 8 February. Operational numerical model guidance appears to be helpful in the analysis and prediction of these downslope winds when used to evaluate the mountain wave potential rather than evidence of the event itself. Model sounding data are particularly useful for examining the predicted change in stability and wind at all levels over time. Time series cross sections of theta (Fig. 11a) and the wind component normal to the mountain ridge (Fig. 11b) provide a good view of the model forecast of stability and critical-level heights, respectively. Further evaluation of other situations that produce mountain wave windstorms is needed to provide additional verification and confidence in this method.

Predicting the end of downslope winds based on a numeric forecast of less favorable atmospheric conditions is also somewhat successful in the 8 February case study. This problem is more difficult however, since it

may be possible for a wave to become significant enough to generate its own ''self-induced'' critical level through wave overturning, and delay its sensitivity to synoptic-scale changes.

Mesoscale analysis provides some insight into the interaction between a mountain wave event and nearby gap flow by detailing areas of increased surface pressure gradient and wind. Since an amplified mountain wave appears to also enhance gap winds, it is not always easy for the forecaster to isolate the cause of these winds. There remains a need for better measurements in the mesoscale as an aid in the analysis and prediction of these windstorm events.

It is encouraging that some NGM numerical products provide information that assists in analyzing and forecasting a synoptic-scale condition leading to downslope windstorms. Newer mesoscale models with increased resolution and more detailed terrain should improve guidance for forecasting these events. However, they will also make it more difficult to determine whether specific parameters were affected by the larger-scale synoptic pattern or by the mesoscale event. As operational model resolution increases, qualitative thresholds with respect to mountain wave criteria should be reevaluated.

Acknowledgments. This work was supported in part by the COMET Outreach program. Thanks to Brad Colman and Dale Durran for their guidance and comments, and to the anonymous reviewers for their helpful ideas and suggestions.

REFERENCES

Brinkmann, W. A. R., 1974: Strong downslope winds at Boulder, Colorado. *Mon. Wea. Rev.,* **102,** 592–602.

Colman, B. R., and C. F. Dierking, 1992: The Taku wind of southeast Alaska: Its identification and prediction. *Wea. Forecasting,* **7,** 49–64.

Durran, D. R., 1986: Another look at downslope windstorms. Part I: On the development of analogs to supercritical flow in an infinitely deep, continuously stratified fluid. *J. Atmos. Sci.,* **43,** 2527–2543.

——, 1990: Mountain waves and downslope winds. *Atmospheric Processes over Complex Terrain, Meteor. Monogr.,* No. 45, Amer. Meteor. Soc., 59–81.

——, and J. B. Klemp, 1987: Another look at downslope windstorms. Part II: Nonlinear amplification beneath wave-overturning layers. *J. Atmos. Sci.,* **44,** 3402–3412.

Klemp, J. B., and D. K. Lilly, 1975: The dynamics of wave induced downslope winds. *J. Atmos. Sci.,* **32,** 320–339.

——, and ——, 1978: Numerical simulation of hydrostatic mountain waves. *J. Atmos. Sci.,* **35,** 78–107.

Overland, J. E., and B. A. Walter Jr., 1981: Gap winds in the Strait of Juan de Fuca. *Mon. Wea. Rev.,* **109,** 2221–2233.

Peltier, W. R., and T. L. Clark, 1979: The evolution and stability of finite-amplitude mountain waves. Part II. Surface wave drag and severe downslope windstorms. *J. Atmos. Sci.,* **36,** 1498–1529.

Smith, R. B., 1985: On severe downslope winds. *J. Atmos. Sci.,* **42,** 2597–2603.

——, and J.-L. Sun, 1987: Generalized hydraulic solutions pertaining to severe downslope winds. *J. Atmos. Sci.,* **44,** 2934–2939.